Evaluation of impedance and teleoperation control of a hydraulic mini-excavator

S.E. Salcudean, S. Tafazoli, K. Hashtrudi-Zaad and P.D. Lawrence
University of British Columbia
Vancouver, Canada
{*tims@ee.ubc.ca*}

C. Reboulet
ONERA-CERT
Toulouse, France

Abstract: A position-based impedance controller has been implemented on a mini-excavator. Its performance and an approach to evaluate its stability robustness for given environment impedances are discussed. A dual hybrid teleoperation controller is proposed for machine control. Issues of transparency are discussed.

1. Introduction

There are hundreds of thousands of excavator-based machines manufactured every year and widely used in the construction, forestry and mining industry. These are four-degree-of-freedom hydraulic arms as illustrated in Figure 1, having a cab "waist" rotation, and three links moving in the vertical plane, called, in order from the cab to the end-effector, the "boom", "stick" and "bucket". The controls and human interfaces of excavator-based machines are still rather primitive. Operators use joysticks or levers to control the extension of the individual cylinders, and not the bucket motion in task space by computer-coordinated cylinder control.

The need for coordinated cylinder control has been demonstrated in [1]. Machine modeling (arm dynamics and hydraulics) and control leading to accurate task-space motion have been discussed in [2]. Individual variable-displacement pump cylinder control has been used for fast, accurate and efficient coordinated motion of a CAT-325 machine [3].

Although the need for control of forces during excavation tasks has not been formally proven, the efficiency of such tasks depends on exerted forces and should be enhanced by force or impedance control of the excavation arm. Limited models of excavators and their interaction with the soil are presented in [4]. Kinematic and dynamic models for such machines assuming that the machine cylinders act as force sources are presented in [5, 6], with [6] adding simplified digging dynamics for digging simulations.

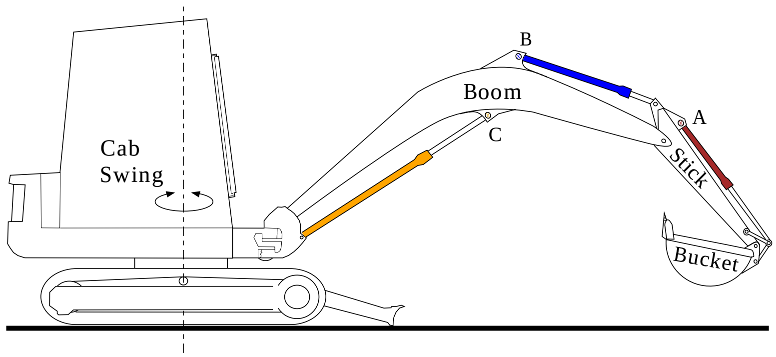

Figure 1. Mini-excavator Schematic.

Force-feedback teleoperated control of excavator-based machines has been reported in [7, 3]. The accomplishment of contact tasks relied entirely on the operator controlling the machine velocity via an active joystick, with stiffness modulated by end-point forces measured via hydraulic cylinder pressures. Since contact forces were controlled in closed loop only by the operator action and force measurements from differential pressure sensing had large errors due to cylinder friction, these results have not been entirely satisfactory.

The control of contact tasks could be improved by some form of impedance control [8] of the excavator arm. Impedance control of hydraulic robots has been presented before (*e.g.*, [9]), but there has been no reported work of the impedance control of an excavator arm. A position-based impedance controller for an excavator arm and experimental results demonstrating impedance control of the stick cylinder are being presented in [10].

In this paper, issues of task-space stiffness/impedance control of an excavator are addressed and the problem of force-feedback teleoperation of excavato-based machines is revisited given this more versatile control mode. The paper is organized as follows: Section 2 briefly presents the mini-excavator used as an experimental base, Section 3 discusses issues of single-cylinder position control, task-space impedance control is presented in Section 4, while teleoperated control is presented in Section 5. Section 6 presents conclusions and future research directions.

2. Instrumented Mini-excavator

A Takeuchi TB035 mini-excavator has been used as a research platform for the experiments presented in this paper. The model and instrumentation for this machine can be found in [11].

Encoders have been installed to measure the cab-boom, boom-stick and stick-bucket angles. Load pins have been installed on the boom, stick and bucket cylinders and measure the boom cylinder force and the reaction forces of the stick and bucket cylinders. The pilot system for the main valves of the arm cylinders have been modified for computer control by using ON/OFF valves operated in differential pulsed-width modulation mode [12, 11]. The use of load-pins allows for much more accurate end-effector force-measurement than cylinder pressures, since joint friction is small and cylinder friction is substantial [13, 11]. A VME-based real-time system with the VxWorks operating system are being used to control the machine.

3. Single cylinder position control

Since the hydraulic cylinders behave like velocity sources, the range of attainable arm impedances is better when a position-based impedance control scheme is used [14]. For this purpose, inner-loop cylinder controllers were implemented with the goal of closely emulating velocity sources.

The controllers utilize compensation for the main spool dead-band, which, for safety reasons, is quite significant in all machines of these type. Proportional-derivative controllers with two sets of gains - one for cylinder extension and one for cylinder contraction - have been found to give satisfactory performance with a commanded to actual position transfer function described approximately by first order linear transfer functions of the form $1/(sT_i + 1)$, where the T_i's are of the order of 0.2 s. Let $l = [l_{boom},\ l_{stick},\ l_{bucket}]^T$, $l_d = [l_{boom\_d},\ l_{stick\_d},\ l_{bucket\_d}]^T$, and $P = diag\{P_1,\ P_2,\ P_3\}$. Experiments demonstrating impedance control of the stick cylinder are presented in [10].

4. Impedance Control

4.1. Impedance model

A desired task-space impedance of the following form is assumed:

$$f_0 - f_e \quad = \quad E_1 x + E_2(x - x_0) = (E_1 + E_2)x - E_2 x_0 \tag{1}$$

where x_0 and x are the desired and actual bucket position, and f_0 and f_e are the desired and actual forces by the bucket *on* the environment. Typically $E_1 = E_1(s) = M_i s^2$ and $E_2 = E_2(s) = M_d s^2 + B_d s + K_d$, where s is the derivative or Laplace operator.

For a task-space environment described by $f_e = E_e x$, the proposed impedance control results in

$$(E_1 + E_2 + E_e)x \quad = \quad E_2 x_0 + f_0 \tag{2}$$

$$(E_1 + E_2 + E_e)E_e^{-1} f_e \quad = \quad f_0 + E_2 x_0 \ , \tag{3}$$

and x tracks x_0 if $\|E_2\| \gg \|E_1 + E_e\|$, while f_e tracks f_0 if $\|E_e\| \gg \|E_1 + E_2\|$.

4.2. Impedance Controller Design

An implementation of (1) can be realized using the linearized excavator arm dynamics and the hydraulics dynamics. The arm dynamics are given by

$$E_r x + J_r^{-T} \tau_g \quad = \quad J^{-T} f_c - f_e \tag{4}$$

where $E_r(s) = M_r s^2$, M_r is the task-space excavator arm mass matrix, τ_g are the arm joint torques due to gravity, f_c are the applied cylinder forces, and

$$\dot{q} = J_c \dot{l}, \quad \dot{x} = J_r \dot{q}, \quad J = J_r J_c \quad , \tag{5}$$

where q is the vector of joint angles. The hydraulics dynamics is described in task space as

$$x = JPJ^{-1} x_d \ . \tag{6}$$

Let the impedance controller be given by

$$x_d = J\hat{P^{-1}} J^{-1} (E_1 + E_2 - E_r)^{-1} (E_2 x_0 + f_0 - J^{-T} f_c + J_r^{-T} \tau_g) \ , \tag{7}$$

or, equivalently,

$$l_d \quad = \quad \hat{P^{-1}} [J^T (E_1 + E_2 - E_r) J]^{-1} [J^T E_2 J l_0 + J^T f_0 - f_c + J_c \tau_g) \ , \tag{8}$$

where $\hat{P^{-1}}(s)$ is a stable approximation to the inverse of $P(s)$. With $G^{-1} = P\hat{P^{-1}}$, the following closed-loop impedance is obtained:

$$f_0 - f_e = [E_r + (E_1 + E_2 - E_r) JGJ^{-1}] x - E_2 x_0 \ . \tag{9}$$

In the above, the Lapace variable s is used as the derivative operator and it is assumed that the arm configuration changes slowly enough for the Jacobian to be considered to be constant (so s and J commute).

In the impedance control law (7), the mass matrix term $E_r = s^2 M_r = s^2 J_r^{-T} D(q, \lambda) J_r^{-1}$ and the gravitational term $J_r^{-T} \tau_g(q, \lambda)$ can be evaluated using J_r, the arm mass matrix D, and the joint torques due to gravity τ_g, evaluated as functions of joint coordinates q and a set of inertial parameters λ. The parameters λ were previously identified using a least-squares fit of joint angle and cylinder force data [13, 11], while $D(q, \lambda)$ was obtained as a symbolic matrix function using Maple.

Note that the closed-loop dynamics (9) reduce to the desired impedance equation (1) when $G = I$. Also note that the control law is significantly simplified if $E_1 = E_r$ in the above. Since, typically, $E_2(s) = M_d s^2 + B_d s + K_d$, with all entries being positive definite, the intended task-space arm impedance will have the same or larger inertia, depending on whether $M_d = 0$ or > 0, so impact forces could not be reduced by this approach. An alternative for impact force reduction is to modify the force set point f_0 to $f_0 + E_f x$, where $E_f = M_f s^2 x$ is an inertia term (since E_f is not proper, a low-pass filter should be added to the inertial term). As long as G is close to the identity and $M_r + M_d - M_f > 0$, the system remains stable in spite of this positive feedback term.

4.3. Stability Analysis

Closed-loop system stability for a particular arm configuration and environment having dynamics $f_e = E_e x$ could be verified by determining whether

$$H = E_e - E_f + E_r + (E_1 + E_2 - E_r) JGJ^{-1} \tag{10}$$

has a stable inverse using the multivariable Nyquist criterion. Guidelines for the choice of impedance parameters can be obtained by considering the scalar equivalent, with $P(s) = 1/(sT_1 + 1)$, $\hat{P}^{-1}(s) = (sT_1 + 1)/(sT + 1))$, $E_e(s) = m_e s^2 + b_e s + k_e$, $E_r(s) = m_r s^2$, $E_f(s) = m_f s^2$, $E_1(s) = m_r s^2$ and $E_2(s) = m_d s^2 + b_d s + k_d$, in which case equation (10) becomes

$$H = [(m_e + m_r - m_f)s^2 + b_e s + k_e] + [m_d s^2 + b_d s + k_d](sT + 1) \ . \tag{11}$$

A sufficient condition for stability is

$$|\frac{(m_e + m_r - m_f)s^2 + b_e s + k_e}{m_d s^2 + b_d s + k_d} \frac{1}{sT + 1}|_{s=j\omega} < 1, \quad \forall \ \omega \ . \tag{12}$$

As long as $m_e + m_r - m_f > 0$, for overdamped environments, choosing a critically damped E_2 is a sufficient condition for stability. For underdamped environments, the impedance parameters have to be selected for significant roll-off of E_2^{-1} before the resonant frequency of the environment.

4.4. Experimental Results

Experiments illustrating the effectiveness of task-space impedance control for a prototype leveling task are presented in this section. In such a task, the operator would move the bucket radially back-and-forth while exerting a normal force on the ground. Thus, the radial position R_t of the bucket tip, the bucket orientation α_t, and the vertical forces f_{ez} against the ground should be controlled. The impedance controller (8) was implemented with $\hat{P}^{-1} = I$ along the elevation axis Z_t, with

$$E_{1Z}(s) = M_r s^2 \quad \text{and} \quad E_{2Z}(s) = 400s^2 + 10,000s + 10,000 \quad . \tag{13}$$

SI units are used throughout.

A piece of wood was laid on the ground in front of the excavator arm at an approximate elevation $Z_t = -1$ m. A desired trajectory as shown in dotted lines in Figure 2 was commanded. Only the bucket tip was in contact with the wood, in accordance with the kinematics and Jacobian calculations used in the controller. Figure 2 shows the bucket trajectory, Figure 3 shows the bucket forces, Figure 4 shows the cylinder extensions, and Figure 5 shows the cylinder forces. Position control results are shown on the left, impedance control results are shown on the right, and commanded trajectories are presented with dashed lines.

The experimental results show that in impedance mode, the bucket trajectory does comply to the environment contraint, transient forces are significantly lower, and steady-state contact forces tend to zero. By contrast, in position control, interaction forces are significantly higher. Note that because the arm does not comply to the constraint, the machine cab tilts up during position control, so the location readings of Figure 2 are in cab-frame, not ground frame.

The present impedance settings actually add to the robot mass by roughly 400 Kg. It is expected that the control law modification suggested in the previous sub-section will help reduce the level of the impact force on the machine.

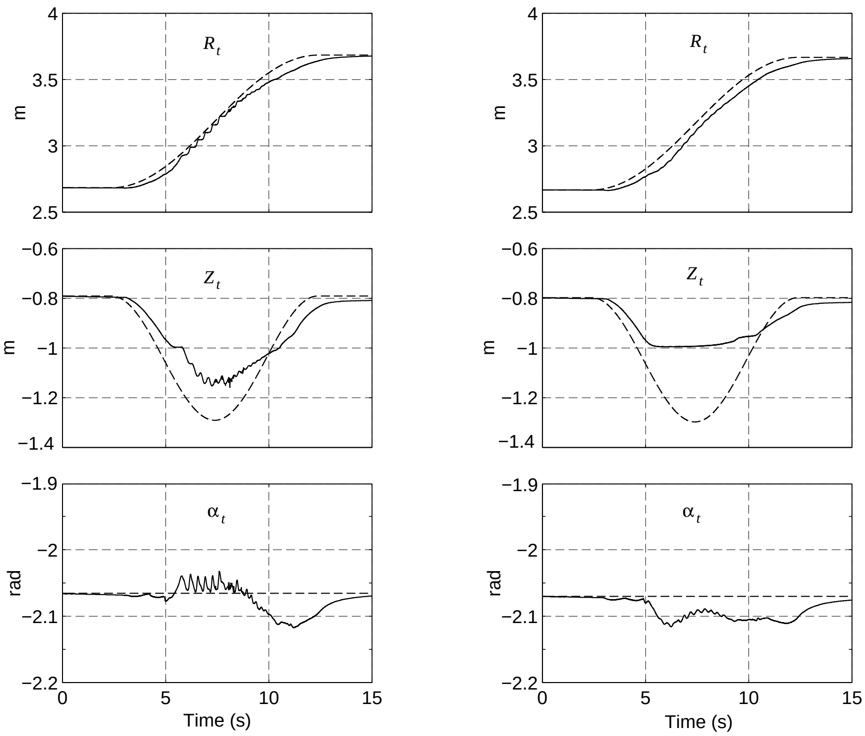

Figure 2. Position tracking in task-space under position and impedance control. Dashed lines show commanded positions.

5. Teleoperation

The existence of an effective impedance control law for the excavator arm allows more sophisticated teleoperation controllers to be implemented than the ones presented in [7, 3]. A four-channel teleoperation system is assumed as described schematically in Figure 6, where the achieved hydraulic arm impedance relationship (9) has been re-written as the "slave manipulator" dynamics

$$(Z_s + C_s)v_s \quad = \quad Z_d v_{s0} + f_{s0} - f_e \ , \tag{14}$$

where $v_s = sx$, $v_{s0} = sx_0$, $f_{s0} = f_0$, $Z_s = E_r/s$, $Z_d = E_2/s$ and $C_s = (E_1 + E_2 - E_r)JGJ^{-1}/s$ is the compensator and the hydraulic dynamics.

The teleoperation master is assumed to be a force-source controlled (PD) mass as follows:

$$(Z_m + C_m)v_m \quad = \quad C_m v_{m0} + f_h + f_{m0} \tag{15}$$

where $Z_m = M_m s^2$ is the master impedance, C_m is a position compensator, f_h is the hand force on the master, and f_{m0} is the master actuator force.

Force and position signals are communicated between the master and the slave, with $v_{s0} = C_1 v_m$, $f_{m0} = -C_2 f_e$, $f_{s0} = C_3 f_h$, $v_{m0} = -C_4 v_s$, and lead to

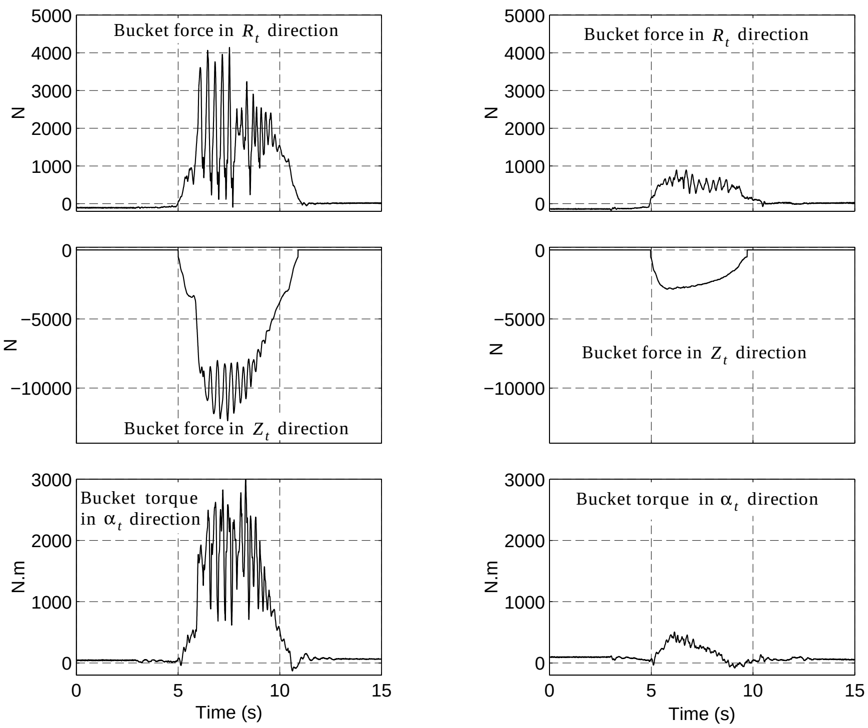

Figure 3. Trajectory forces (torques by the bucket tip).

the following teleoperation system dynamics:

$$\begin{array}{rcrcrcl} -C_m C_4 v_s & + & f_h & = & (Z_m + C_m) v_m & + & C_2 f_e \\ (Z_s + C_s) v_s & - & C_3 f_h & = & Z_d C_1 v_m & - & f_e \end{array} . \tag{16}$$

5.1. Transparency and Dual Hybrid Teleoperation

Equation (16) can be solved for v_s and f_h in terms of v_m and f_e in hybrid matrix form [15, 16]:

$$\begin{bmatrix} f_h \\ -v_s \end{bmatrix} = \begin{bmatrix} Z_{m0} & G_f^{-1} \\ G_p & Z_{s0}^{-1} \end{bmatrix} \begin{bmatrix} v_m \\ f_e \end{bmatrix} . \tag{17}$$

If $f_e = Z_e v_s$, the impedance transmitted to the operator's hand $f_h = Z_{th} v_m$ is given by

$$Z_{th} = Z_{m0} - G_f^{-1} Z_e (I + Z_{s0}^{-1} Z_e)^{-1} G_p \tag{18}$$

$$Z_{m0} - G_f^{-1} (Z_e^{-1} + Z_{s0}^{-1})^{-1} G_p \tag{19}$$

and, in terms of the parameters in (16), by

$$\begin{aligned} Z_{th} = & [I - (C_2 Z_e + C_m C_4)(Z_s + C_s + Z_e)^{-1} C_3]^{-1} \times \\ & [(C_2 Z_e + C_m C_4)(Z_s + C_s + Z_e)^{-1} Z_d C_1 + (Z_m + C_m)] . \end{aligned} \tag{20}$$

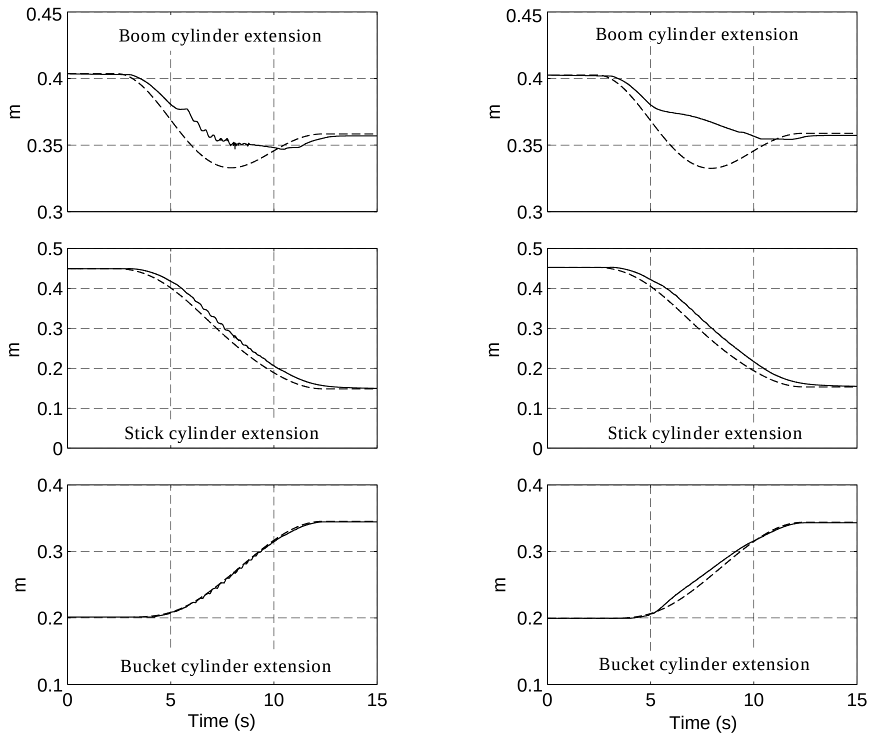

Figure 4. Cylinder extensions. Dashed lines show commanded extensions.

The teleoperation system is *transparent* if the slave follows the master, i.e., $G_p = I$ for position control and $G_p = I/s$ for rate control, and if Z_{th} is equal to Z_e for any environment impedance Z_e [15, 16, 17] (or, alternatively, $Z_{th} = Z_{t0} + Z_e$, where Z_{t0} is a "tool" impedance, usually taken to be Z_m [17]).

In special cases, such as identical master and slave dynamics, it is possible to design *fixed controlers* that provide *perfect* transparency [16], even when the slave manipulator is controlled by the master in velocity mode [17]. However, controller design is difficult (all teleoperation "channels", C_mC_1, C_2,C_3 and Z_dC_4 must be non-zero) and the stability robustness is quite poor. As an alternative, techniques using environment identification have been proposed [18] based on the architecture presented in [15]. Such schemes rely upon the identification of the environment impedance and its duplication at the master by adjusting C_m. At least with conventional identification approaches, it was found that environment identification converges slowly [18], has high sensitivity to delays, and therefore is unsuitable when the environment changes fast, as is the case when manipulating constrained objects.

For directions in which Z_e is known, the environment impedance does not need to be identified. In particular, in directions in which Z_e is known to be small (*e.g.,* free-motion), the master should act as a force source/position sensor and have low impedance, while the slave should behave as a position

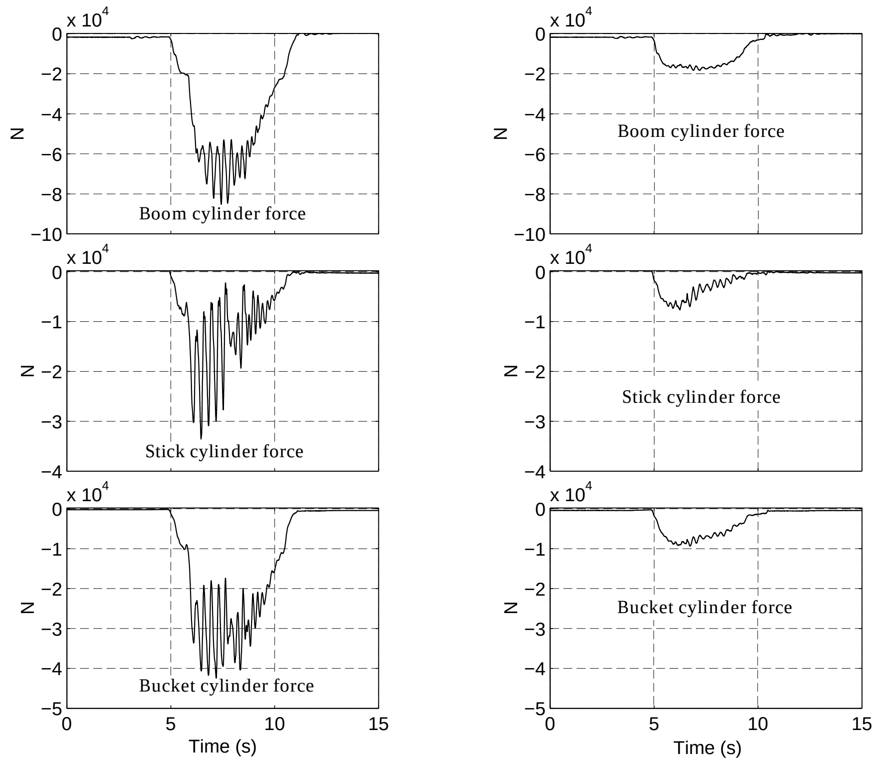

Figure 5. Net forces applied by the cylinders (load-pin reading minus gravity forces.

source/force sensor and have high impedance. Thus, in directions in which Z_e is small, positions are sent to the slave and forces are returned to the master, with C_1 and C_2 having unity transmission, and C_3, C_4 having zero transmission. The dual situation applies in directions in which Z_e is known to be large, (*e.g.,* stiff contact or constraints). In those directions, the master should act as a force sensor/position source and have high impedance, with forces being sent to the slave and positions being returned to the master. Thus, in directions in which Z_e is large, C_1 and C_2 should have zero transmission, while C_3 and C_4 should be close to unity. From (20), it can be seen that the above insures that along very small or very large values of Z_e, the transmitted impedance equals that of the master $Z_m + C_m$, which can be set to the minimum or maximum achievable along required directions.

This concept of "dual hybrid teleoperation" has been introduced, studied and demonstrated experimentally in [19]. It has been shown that when the geometric constraints for a teleoperation task are known, the master and slave workspaces can be split into dual position-controlled and force-controlled subspaces, and information can be transmitted unilaterally in these orthogonal subspaces, while still providing useful kinesthetic feedback to the operator [19].

Consider the case of the leveling task discussed before. When the excavator

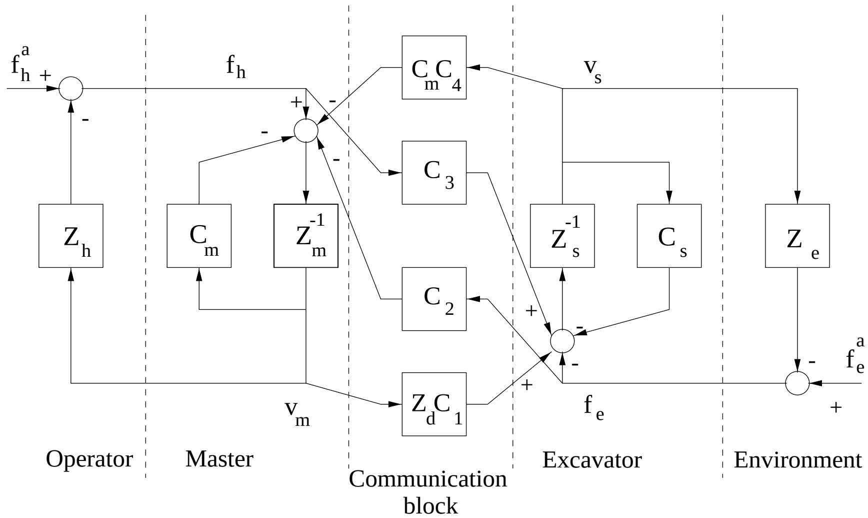

Figure 6. Four-channel teleoperation system.

bucket approaches the ground following the master position or velocity, it is controlled in position or rate mode. The master acts as a position sensor in the radial, axial and bucket orientation directions. Once contact of the bucket with the ground is detected, along the elevation axis the master impedance is set to a high value, while the excavator impedance is set to a low value. The master becomes a force sensor along this axis, with the sensed force being sent to the slave as an elevation axis force command.

5.2. Experimental results

A six-degree-of-freedom magnetically levitated wrist [20] is being used as a teleoperation master for controlling velocity and forces. The leveling experiment discussed above will be carried out and reported in the near future.

6. Conclusion

Position-based impedance control of an excavator arm has been proposed, implemented and experimentally evaluated. In a prototype leveling task, it was shown that contact forces are substantially reduced, and the excavator arm stiffness is close to the one designed for. The use of impedance control to teleoperate the excavator in dual hybrid mode has been discussed.

This is the first time that the compliant control of an excavator arm has been reported. Applications of the technology are bound to follow, but there is much work yet to be done for the seamless integration of teleoperation with and without force feedback in the operation of such machines. This includes better position control of the indvidual cylinders, impedance identification for use in teleoperated control, and haptographical user interfaces to facilitate operation.

7. Acknowledgements

The authors wish to thank Icarus Chau for help with software development and Simon Bachmann for help with the hydraulics system. This work was has been supported by the Canadian NCE IRIS Project IS-4 and associated BC Infrastructure funds.

References

[1] U. Wallersteiner, P. Stager, and P.D. Lawrence, "A human factors evaluation of teleoperated hand controllers," in *International Symposium on Teleoperation and Control*, (Bristol, England), July 1988.

[2] N. Sepehri, P.D. Lawrence, F. Sassani and R. Frenette, "Resolved-mode teleoperated control of heavy-duty hydraulic machines," *Journal of Dynamic Systems, Measurement and Control*, vol. 116, pp. 232–240, June 1994.

[3] P.D.Lawrence, S.E. Salcudean, N. Sepehri, D. Chan, S. Bachmann, N. Parker, M. Zhu and R. Frenette, "Coordinated and force-feedback control of hydraulic excavators," in *Experimental Robotics IV, The Fourth International Symposium, Stanford Ca., June 30-July 2, 1995*, pp. 181–194, Springer Verlag, 1996.

[4] Alekseeva, T.V., Artem'ev, K.A., Bromberg, A.A., Voitsekhouskii, R.I., and Ul'yanov, N.A., *Machines for Earthmoving Work: Theory and Calculations.* New Delhi, India: Amerind Publishing Co., Pvt. Ltd., 1985.

[5] Vaha, P. K. and Skibniewski, M. J., "Dynamic Model of Excavator," *Journal of aerospace engineering.*, vol. 6, pp. 148–158, April 1993.

[6] Koivo, A J, Thoma, M, Kocaoglan, E, and Andrade-Cetto, J., "Modeling and control of excavator dynamics during digging operation," *Journal of aerospace engineering.*, vol. 9, no. 1, pp. 10–18, 1996.

[7] N.R. Parker, S.E. Salcudean, and P.D. Lawrence, "Application of Force Feedback to Heavy Duty Hydraulic Machines," in *Proceedings of the IEEE International Conference on Robotics and Automation*, (Atlanta, USA), pp. 375–381, May 2-6, 1993.

[8] N. Hogan, "Impedance control: An approach to manipulation, parts i-iii," *ASME J. of Dynamic Systems, Measurement, and Control*, vol. 107, pp. 1–23, March 1985.

[9] N. S. B. Heinrichs and A. Thornton-Trump, "Position-based impedance control of an industrial hydraulic manipulator," *IEEE Contr.Sys. Mag.*, vol. 17, pp. 46–52, February 1997.

[10] S.E. Salcudean, S. Tafazoli, P.D. Lawrence and I. Chau, "Impedance control of a teleoperated mini excavator," in *Proc. 1997 ICAR*, June 1997. to appear.

[11] S. Tafazoli, *Identification of frictional effects and structural dynamics for improved control of hydraulic manipulators.* PhD thesis, University of British Columbia, January 1997.

[12] S. Tafazoli, P. Peussa, P.D. Lawrence, S.E. Salcudean, and C.W. de Silva, "Differential pwm operated solenoid valves in the pilot stage of mini excavators: modeling and identification," in *Proc. ASME Int. Mech. Eng. Congr. and Expo., FPST-3*, (Atlanta, GA), pp. 93–99, November 1996.

[13] S. Tafazoli, P.D. Lawrence, S.E. Salcudean, D. Chan, S.Bachmann and C.W. de Silva, "Parameter estimation and friction analysis for a mini excavator," in *Proc. IEEE Int. Conf. on Robotics and Automation*, vol. 1, (Minneapolis, Minnesota), pp. 329–334, April 1996.

[14] D. Lawrence, "Impedance control stability properties in common implementations," in *Proc. IEEE Int. Conf. Rob. Aut.*, pp. 1185–1190, March 1988.

[15] B. Hannaford, "A Design Framework for Teleoperators with Kinesthetic Feedback," *IEEE Transactions on Robotics and Automation*, vol. RA-5, pp. 426–434, August 1989.

[16] D. A. Lawrence, "Designing Teleoperator Architecture for Transparency," in *Proceedings of the IEEE International Conference on Robotics and Automation*, (Nice, France), pp. 1406–1411, May 10-15 1992.

[17] M. Zhu and S. Salcudean, "Achieving transparency for teleoperator systems under position and rate control," in *Proceedings of the 1995 IEEE/RSJ International Conference on Intelligent Robots and Systems (IROS'95)*, (Pittsburgh, PA), August 5-9 1995.

[18] K. Hashtrudi Zaad and S.E. Salcudean, "Adaptive transparent impedance reflecting teleoperation," in *Proc. IEEE International Conference on Robotics and Automation*, (Minneapolis, Minnesota), pp. 1369–1374, April 22-28 1996.

[19] C. Reboulet, Y. Plihon and Y. Briere, "Interest of the dual hybrid control scheme for teleoperation with time delays," in *Experimental Robotics IV, The Fourth International Symposium, Stanford Ca., June 30-July 2, 1995*, pp. 498–506, Springer Verlag, 1996.

[20] S.E. Salcudean and N.M. Wong, "Coarse-fine motion coordination and control of a teleoperation system with magnetically levitated master and wrist," in *Third International Symposium on Experimental Robotics*, (Kyoto, Japan), Oct 28-30, 1993.